

This is the accepted peer-reviewed manuscript (postprint) of "Assessing pyrite-derived sulfate in the Mississippi River with four years of sulfur and triple-oxygen isotope data" by Bryan Killingsworth (bryan.a.killingsworth(at)gmail.com), Huiming Bao, and Issaku Kohl

The final, copy-edited, version was published in Environmental Science & Technology and can be found at <https://doi.org/10.1021/acs.est.7b05792>

This postprint was provided by the publisher as a courtesy for the fulfillment of funder open access requirements and is submitted to EarthArXiv by the authors.

1 Assessing pyrite-derived sulfate in the Mississippi River with four years of sulfur and 2 triple-oxygen isotope data

3

4 Bryan A. Killingsworth^{a,b,*}, Huiming Bao^a, and Issaku E. Kohl^{a,\$}

5

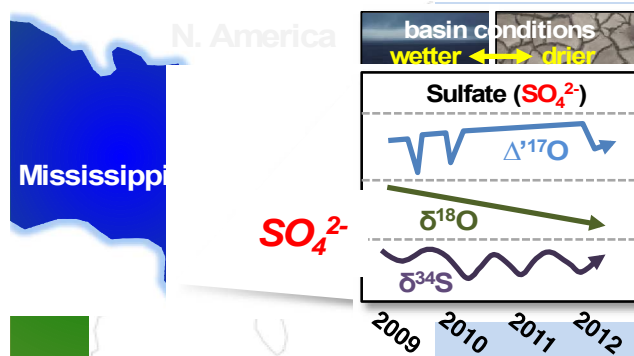
6 ^aDepartment of Geology & Geophysics, Louisiana State University, Baton Rouge, Louisiana7 70803, United States; ^bIUEM, Laboratoire Géosciences Océan, Université de Bretagne8 Occidentale, UMR 6538, Plouzané 29280, France; ^{\$}Department of Earth, Planetary, and Space

9 Sciences, University of California Los Angeles, Los Angeles 90095, California, United States

10

11 **Abstract**

12 Riverine dissolved sulfate (SO_4^{2-})
13 sulfur and oxygen isotope variations
14 reflect their controls such as SO_4^{2-}
15 reduction and re-oxidation, and source
16 mixing. However, unconstrained temporal
17 variability of riverine SO_4^{2-} isotope
18 compositions due to short sampling
19 durations may lead to mischaracterization
20 of SO_4^{2-} sources, particularly for the
21 pyrite-derived sulfate load. We measured



22 the sulfur and triple-oxygen isotopes ($\delta^{34}\text{S}$,
23 $\delta^{18}\text{O}$, and $\Delta^{17}\text{O}$) of Mississippi River SO_4^{2-} with biweekly sampling between 2009-2013 to test
24 isotopic variability and constrain sources. Sulfate $\delta^{34}\text{S}$ and $\delta^{18}\text{O}$ ranged from -6.3‰ to -0.2‰
25 and -3.6‰ to $+8.8\text{‰}$, respectively. Our sampling period captured the most severe flooding and
26 drought in the Mississippi River basin since 1927 and 1956, respectively, and a first year of
27 sampling that was unrepresentative of long-term average SO_4^{2-} . The $\delta^{34}\text{S}_{\text{SO}_4}$ data indicate pyrite-
28 derived SO_4^{2-} sources are $74 \pm 10\%$ of the Mississippi River sulfate budget. Furthermore, pyrite
29 oxidation is implicated as the dominant process supplying SO_4^{2-} to the Mississippi River,
30 whereas the $\Delta^{17}\text{O}_{\text{SO}_4}$ data shows $18 \pm 9\%$ of oxygen in this sulfate is sourced from air O_2 .

31

32

33

34 **Introduction**

35 The characterization of riverine chemical fluxes today is important for establishing
36 natural baselines for understanding the magnitude of human impact on chemical cycles and
37 interpreting the rock record of biogeochemical changes in Earth's past. For the surface sulfur
38 cycle, which is closely linked to the carbon and oxygen cycles over long time scales, its most
39 significant flux is riverine sulfate input to the ocean¹. Natural variations in the magnitude and
40 isotopic composition of the sulfate flux reflects the exposures and weathering rates of sulfide and
41 sulfate minerals in rocks². Meanwhile, human activities, such as the mining and burning of fossil
42 fuels like coal, can increase riverine sulfate fluxes four-fold and alter sulfate's sulfur isotope
43 composition on a large scale, such as in the Mississippi River³. Thus, studies of the continental
44 sulfur cycle have made efforts to constrain riverine SO_4^{2-} fluxes and isotope compositions
45 globally⁴⁻⁷ and in large⁸⁻¹⁰ and small¹¹⁻¹⁴ rivers. Riverine studies have suggested that global
46 sulfate budgets may underrepresent the pyrite-derived sulfate flux, which is particularly
47 important for sulfur and carbon weathering budgets^{9, 15}.

48 An advantage of riverine chemical studies is their integration of spatial and temporal
49 scales. Depending on the research focus, sampling campaigns of different durations can be
50 designed according to the basin size and its assumed variability, to constrain temporal variation
51 with multi-year sampling, or to reveal spatial variations. However, a lack of temporal constraints
52 on SO_4^{2-} isotopes may result in biased conclusions about sulfate sources and processes. For
53 example, the average isotope compositions of inputs are needed to construct stable isotope
54 mixing models to constrain sulfate sources in individual rivers and in models of the global
55 surface sulfur cycle. A low frequency or short duration of sampling may bias model results
56 towards one season or an anomalous year. Only some riverine sulfate isotope studies last a year⁸.

57 ^{10, 16-18} or longer¹⁹⁻²⁶, and out of the rivers that were monitored for ≥ 1 year, just the Yangtze,
58 Indus, Oldman, and Kalix are $>5,000 \text{ km}^2$. For these long-term studies, the average ranges for
59 $\delta^{34}\text{S}$ and $\delta^{18}\text{O}$ are $\sim 5\text{‰}$ and have no correlation with catchment size. Thus there are insufficient
60 temporal constraints on riverine SO_4^{2-} isotope variability over large, and continental, spatial
61 scales. For example, significant variability was shown within one year of Yangtze River sulfate
62 data where the ranges of $\delta^{34}\text{S}_{\text{SO}_4}$ and $\delta^{18}\text{O}_{\text{SO}_4}$ were respectively 9.5‰ and 8.9‰ ¹⁰. In another
63 example from a highly cited study, $85\% \pm 5\%$ of sulfate flux in the relatively pristine Mackenzie
64 River in Canada was attributed to pyrite oxidation⁹. This assessment was based on stable isotope
65 ($\delta^{34}\text{S}$ and $\delta^{18}\text{O}$) mixing of sulfate sources for 20 samples taken throughout the basin at one time,
66 with only one sample recovered from the river mouth that could represent the output to the
67 ocean. The respective $\delta^{34}\text{S}$ and $\delta^{18}\text{O}$ had significant spatial variation of 28.3‰ and 12.6‰ ,
68 respectively, and the temporal variability was undetermined. While the conclusion appears
69 robust that most of the sulfate in the Mackenzie is pyrite-derived, it remains difficult to know if
70 the estimate of pyrite-derived sulfate flux is applicable to the long term. Regardless, the
71 estimation of pyrite-derived sulfate loads, and its natural and anthropogenic partitioning, is not a
72 trivial task due to large $\delta^{34}\text{S}$ and $\delta^{18}\text{O}$ ranges and their overlaps with other sulfate sources. High
73 loadings of pyrite-derived sulfate may result in large ranges of $\delta^{34}\text{S}_{\text{SO}_4}$ and $\delta^{18}\text{O}_{\text{SO}_4}$, which are
74 commonly used as sulfate source tracers. Regardless, a lack of significant temporal variability,
75 and a coupled response related to sources, are implicitly assumed for $\delta^{34}\text{S}_{\text{SO}_4}$ and $\delta^{18}\text{O}_{\text{SO}_4}$.



76

77 **Figure 1.** The Mississippi River basin within the contiguous United States, with the Missouri
78 and Ohio River sub-basins and the sampling location for this study at Baton Rouge, Louisiana
79 identified. Image is modified from the original from NASA/JPL²⁷.

80

81 To test SO_4^{2-} isotopic variability over time and constrain sources, we target the
82 Mississippi River. The Mississippi, Yangtze, and Amazon Rivers are the top three rivers for
83 sulfate flux to the ocean worldwide²⁸. The Mississippi River basin (Figure 1) covers ~37% of the
84 contiguous United States²⁹ and is the largest river system in North America. The Mississippi
85 River basin has been heavily altered by human activities such as agriculture (65% by area³⁰),
86 dams and reservoirs in the semi-arid west, and levee systems prevalent in the lower Mississippi
87 River. Bedrock sources of sulfate within the Mississippi River include abundant pyrite-bearing
88 shales in its western reaches, evaporite exposures, and mine drainage from coalbeds within sub-
89 basins in the west (Missouri River) and east (Ohio River). The Mississippi River $\delta^{34}\text{S}_{\text{SO}_4}$ average
90 was previously used in a stable isotope mixing model to characterize sulfate sources³, whereas
91 the full time series $\delta^{34}\text{S}_{\text{SO}_4}$, $\delta^{18}\text{O}_{\text{SO}_4}$, and $\Delta^{17}\text{O}_{\text{SO}_4}$ data from 2009-2013 are reported here. In the
92 previous study, it was estimated that human activities account for 75% of the Mississippi River
93 SO_4^{2-} flux and have increased the average Mississippi River $\delta^{34}\text{S}_{\text{SO}_4}$ from -5% to -2.7% , and it

94 was concluded that the more typical scenario should be the opposite – where most rivers should
95 instead display decreasing $\delta^{34}\text{S}_{\text{SO}_4}$ due to human influence. The distinctly low $\delta^{34}\text{S}_{\text{SO}_4}$ of the
96 Mississippi River was interpreted as the result of a high input of sulfate from the weathering of
97 pyrite. Mississippi River sulfate was partitioned into sources from coalmine drainage (47%),
98 natural and anthropogenic rock weathering (37%), atmospheric sulfur (15%), and fertilizer (1%).
99 In the present study, Mississippi River SO_4^{2-} isotope compositions are compared to ion
100 concentrations, discharge, and temperature from the USGS³¹ and discharge from the USACE³².
101 While average Mississippi River $\delta^{34}\text{S}_{\text{SO}_4}$ made the previous source partitioning possible, four
102 years of data from 2009-2013 permits us to examine the full variability and controls on $\delta^{34}\text{S}_{\text{SO}_4}$,
103 $\delta^{18}\text{O}_{\text{SO}_4}$, and $\Delta^{17}\text{O}_{\text{SO}_4}$ and attempt to more finely resolve the pyrite-derived sulfate load here.

104

105 **Materials and Methods**

106 Mississippi River water was collected biweekly or at greater frequency during the period
107 03/11/09 to 01/17/13 for $\delta^{34}\text{S}_{\text{SO}_4}$, $\delta^{18}\text{O}_{\text{SO}_4}$, and $\Delta^{17}\text{O}_{\text{SO}_4}$ measurements. River water samples
108 were collected at the east bank of the Mississippi River at Baton Rouge or St. Francisville,
109 Louisiana, USA and immediately processed or refrigerated for later processing. Our sampling
110 locations near Baton Rouge, Louisiana integrate the main sub-basins of the Mississippi River
111 except for the Red and Ouachita Rivers, and thus here the SO_4^{2-} flux to the ocean for ~37% of
112 the contiguous United States is accounted for.²⁹ A few additional samples were collected from
113 the sub-basin upper Ohio River at Tell City, Indiana to compare against the main Mississippi
114 River. All samples were treated with the DDARP method, yielding purified BaSO_4 ³³.

115 The riverine dissolved sulfates were analyzed for their isotope $\delta^{34}\text{S}_{\text{SO}_4}$, $\delta^{18}\text{O}_{\text{SO}_4}$, and
116 $\Delta^{17}\text{O}_{\text{SO}_4}$ per the methods here with additional details in the supporting information (chapter 1).

117 The classical isotope notation is used here:

$$118 \quad \delta \equiv R_{\text{sample}}/R_{\text{standard}} - 1 \quad (1)$$

119 Where R is the mole ratio of $^{18}\text{O}/^{16}\text{O}$, $^{17}\text{O}/^{16}\text{O}$, or $^{34}\text{O}/^{32}\text{O}$ and reported in units per mille (\times
120 1000‰) with respect to the international isotope standards VSMOW or VCDT for $\delta^{18}\text{O}$ and $\delta^{34}\text{S}$,
121 respectively. We note that the linear “capital delta” definition is

$$122 \quad \Delta^{17}\text{O} \equiv \delta^{17}\text{O} - C \times \delta^{18}\text{O}, \quad (2)$$

123 where C is an arbitrary reference slope³⁴. Here we use a logarithmic definition,

$$124 \quad \Delta^{17}\text{O} \equiv \delta^{17}\text{O} - C \times \delta^{18}\text{O}, \text{ where} \quad (3)$$

$$125 \quad \delta^{1x}\text{O} = \ln(\delta^{1x}\text{O} + 1) = \ln(R_{\text{sample}}/R_{\text{standard}}). \quad (4)$$

126 The ^{1x}O in equation (4) refers to the isotope ^{18}O or ^{17}O , and $\Delta^{17}\text{O}$ is reported in ‰ with respect
127 to the standard VSMOW (Fig. S1). The choice of the reference slope C in equation (3) is 0.5305,
128 which benefits inter-species comparison³⁴. All measurements for $\Delta^{17}\text{O}$ were done on samples
129 converted to O_2 and run on a Thermo Finnigan MAT 253 isotope ratio mass spectrometer
130 (IRMS) at Louisiana State University (LSU). The raw average of replicate $\delta^{17}\text{O}_{\text{SO}_4}$ and $\delta^{18}\text{O}_{\text{SO}_4}$
131 values (in ‰) are available in Tables S1 and S2 for re-normalization to other reference frames of
132 choice. The $\delta^{34}\text{S}_{\text{SO}_4}$ measurements were conducted at the University of Maryland and Indiana
133 University using an Elemental Analyzer coupled to an IRMS. For $\delta^{18}\text{O}_{\text{SO}_4}$, analysis was done at
134 LSU using a high temperature conversion Elemental Analyzer (TCEA) coupled to a Thermo
135 Finnigan MAT 253 IRMS in continuous flow mode. Analytical errors for standards and sample
136 duplicates for $\delta^{34}\text{S}_{\text{SO}_4}$, $\delta^{18}\text{O}_{\text{SO}_4}$, and $\Delta^{17}\text{O}_{\text{SO}_4}$ are $\pm 0.3\%$, $\pm 0.5\%$, and $\pm 0.05\%$ respectively.

137 To determine trends and seasonality of sulfate, monthly averages of the isotope data were
138 used for time series decomposition in the software “R”³⁵ (Figs. S2 and S3), and sulfate fluxes for
139 the main Mississippi River and sub-basins were compared. Additional available data is used
140 from continuously monitored water discharge, ion concentration, temperature, and other
141 parameters at St. Francisville, Louisiana³¹, where for that location the main stem water discharge
142 of the Mississippi is represented by the Tarbert Landing, MS and Knox Landing, LA sites
143 monitored by the USACE³². Mississippi River sub-basin sulfate concentration and river
144 discharge data is used from the Missouri River at Hermann, MO, Upper Mississippi below
145 Grafton, IL, and Ohio River at Metropolis, IL, which are monitored by the USGS³¹.

146 Sulfate flux estimates for the Mississippi River and its sub-basins use the daily river
147 discharge data with sulfate concentrations reported by the USGS for the respective sites given
148 above. To estimate daily sulfate fluxes for the purposes of matching datasets and making mixing
149 models, sulfate concentrations are interpolated from the approximately once-monthly
150 measurements from the USGS, and matched with daily water discharge reported by the USACE
151 and USGS. Sulfate flux estimates should be considered to have lower resolution than the isotope
152 data due to interpolation from approximate once-monthly concentration measurements.

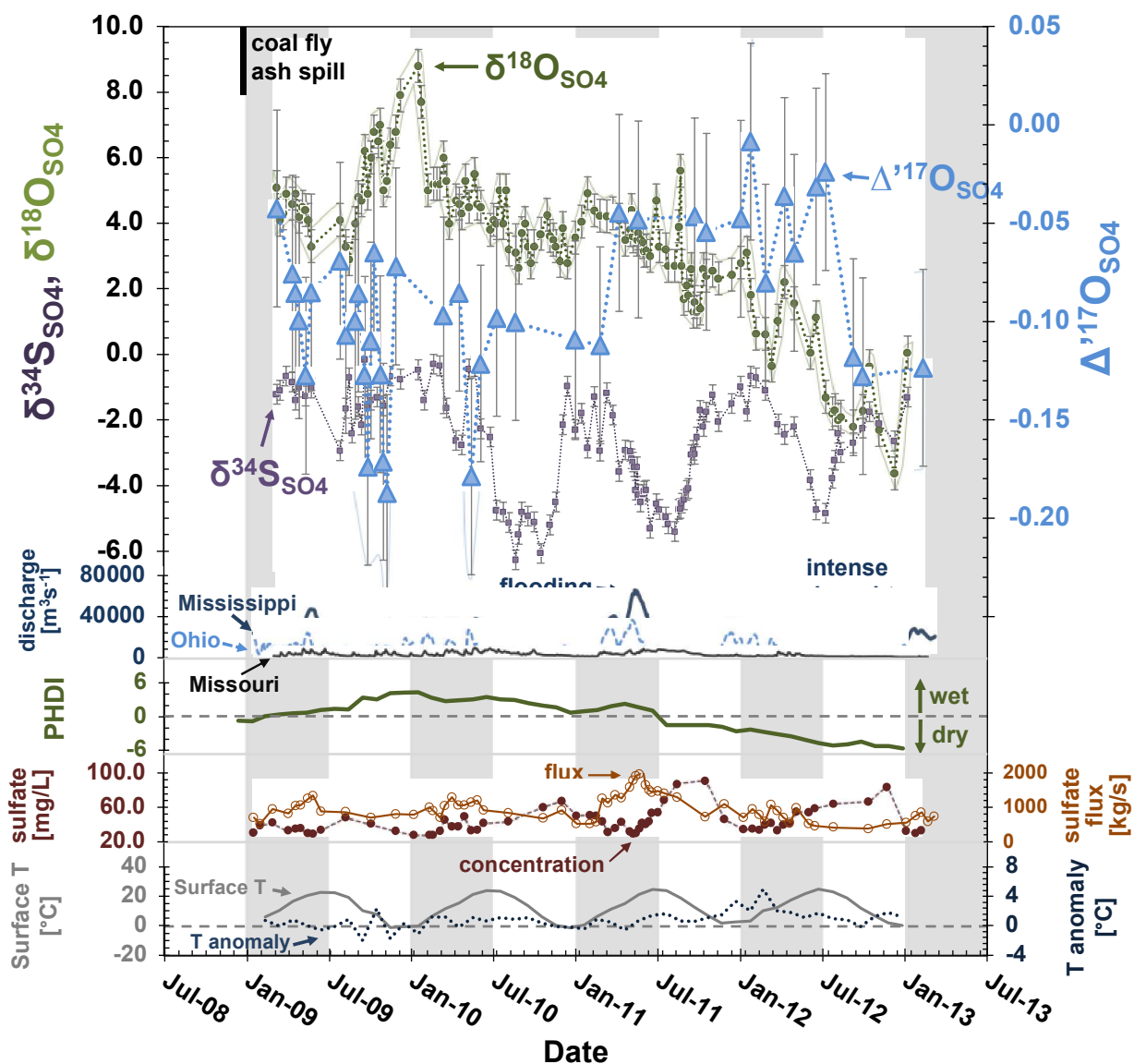
153

154 **Results**

155 Mississippi River SO_4^{2-} varies from -6.3 to -0.2‰ and averages -2.7‰ for $\delta^{34}\text{S}_{\text{SO}_4}$,
156 from -3.6 to 8.8‰ and averages 3.4‰ for $\delta^{18}\text{O}_{\text{SO}_4}$, and ranges -0.19 to -0.01‰ with an average
157 of -0.09‰ for $\Delta^{17}\text{O}_{\text{SO}_4}$ (Figure 2, Table S1). Time series decomposition reveals seasonality in
158 $\delta^{34}\text{S}_{\text{SO}_4}$ with an amplitude of 3‰ , with minima in late summer, and a $\delta^{18}\text{O}_{\text{SO}_4}$ decrease of 5‰

159 from 2009 to 2013 (Figure S2), with $\Delta^{17}\text{O}_{\text{SO}_4}$ exhibiting more secular variation. Histograms of
 160 $\delta^{34}\text{S}_{\text{SO}_4}$ and $\delta^{18}\text{O}_{\text{SO}_4}$ are shown in the supporting information (Fig. S3).

161 Sulfate for the period 01/27/11 to 06/01/11 from the Upper Ohio River sub-basin ranged
 162 from -0.3 to 1.6‰ and averaged 0.3‰ for $\delta^{34}\text{S}_{\text{SO}_4}$ and ranged 1.4 to 2.9‰ and averaged 2.1‰
 163 for $\delta^{18}\text{O}_{\text{SO}_4}$ (Table S2).



164

165

166

167

168 **Figure 2.** Mississippi River sulfate isotope $\delta^{34}\text{S}_{\text{SO}_4}$, $\delta^{18}\text{O}_{\text{SO}_4}$, and $\Delta^{17}\text{O}_{\text{SO}_4}$ data from this study
169 plotted with available data for surface temperature, temperature anomaly (based on monthly
170 averages from 1901-2000), and Palmer Hydrological Drought Index (PHDI) for the contiguous
171 United States³⁶, river basin discharge data^{31, 32}, and sulfate concentration³¹. Sulfate flux is
172 calculated from discharge data and sulfate concentration. Analytical errors for isotope data are
173 shown as error bars and envelopes. Significant events are noted: 1) the Kingston Fossil Plant coal
174 fly ash slurry spill on 12/22/08, 2) historical flooding (the most intense since 1927) in the spring
175 of 2011, and 3) historical drought (strongest since 1956) in the summer to fall of 2012.
176
177

178 **Discussion**

179

180 **Constraining temporal variability**

181 Mississippi River sulfate had higher average $\delta^{34}\text{S}_{\text{SO}_4}$ and an attenuated seasonality in
182 2009 that appear unrepresentative of the long term. The year 2009 may be atypical for two
183 reasons: one of the largest coal fly ash spills in United States history occurred in December 2008
184 where 4.1 million cubic meters of coal ash was released within a tributary of the Mississippi
185 River³⁷, and the summer of 2009 was wetter than average (see PHDI in Fig. 2). Mississippi River
186 sulfate concentrations did not increase due to the coal ash spill although there were modest
187 increases in the tributary where the spill occurred³⁷. The lack of a clear sulfate signal in the
188 Mississippi River from such a spill suggests that widespread coal ash impoundments leaking in
189 the humid southeastern United States³⁸ may contribute diffuse but large fluxes of sulfate that are
190 difficult to quantify. The mixing model used in the previous study was based on the 4-year
191 Mississippi River $\delta^{34}\text{S}_{\text{SO}_4}$ average of -2.7‰ and gave a solution of -5‰ for the $\delta^{34}\text{S}_{\text{SO}_4}$ of
192 natural (pre-anthropogenic) sulfate³. Natural Mississippi River $\delta^{34}\text{S}_{\text{SO}_4}$ would be -0.8‰ from the
193 same model if the 2009 Mississippi River $\delta^{34}\text{S}_{\text{SO}_4}$ average of -1‰ is used. And again, a solution
194 based on the lowest Mississippi River $\delta^{34}\text{S}_{\text{SO}_4}$ of -6.3‰ from 08/26/2010 would imply that
195 natural Mississippi River $\delta^{34}\text{S}_{\text{SO}_4}$ was -14.0‰ . This exercise shows how source estimates can

196 significantly differ from the long term when based on an unrepresentative year or a one-time
197 “snapshot”.

198

199 **Low $\delta^{34}\text{S}$ values of Mississippi River sulfate**

200 The likely source of Mississippi River sulfate with low $\delta^{34}\text{S}_{\text{SO}_4}$ indicated from the
201 Missouri River sub-basin is the weathering of pyrite in rocks deposited during the transgression
202 of a Cretaceous-age epicontinental seaway³ which are now exposed in western and upper reaches
203 of the Mississippi River basin³⁹. The $\delta^{34}\text{S}$ of pyrites in Cretaceous shales can span a wide range,
204 with reported values between +16.7‰ to -34.7‰ but mostly negative with a mean at -19.7‰⁴⁰.
205 The implication for respectively lower and higher $\delta^{34}\text{S}_{\text{SO}_4}$ of the Missouri River and Ohio River
206 is consistent with the seasonal and spatial patterns in $\delta^{34}\text{S}$ from zebra mussels across the
207 Mississippi River basin during 1997-1998⁴¹. The zebra mussel sulfur is sourced from riverine
208 sulfate but slightly fractionated, for example at Baton Rouge the reported mussel $\delta^{34}\text{S}$ was near
209 -4‰ versus the average $\delta^{34}\text{S}_{\text{SO}_4}$ around -3‰ from our study, with their comparison suggesting
210 that Mississippi River sulfate end members have not changed significantly over the past ~20
211 years.

212

213 **Mass balance of pyrite-derived sulfate**

214 Here we provide a more detailed Mississippi River sulfate mass balance that expands on
215 the previous work using the $\delta^{34}\text{S}_{\text{SO}_4}$ average³. The $\delta^{34}\text{S}$ of sulfate from rock weathering of shale
216 pyrite and evaporite (excluding mine drainage), which here we will call $\delta^{34}\text{S}_{\text{RW}}$, was previously
217 estimated as -6.5‰, where the sulfate from natural and anthropogenically enhanced rock
218 weathering were assumed to have the same $\delta^{34}\text{S}$ value³. We adopt $\delta^{34}\text{S}$ values of 20‰ for

219 evaporite⁹ and -17‰ for pyrite from marine shales⁴², for $\delta^{34}\text{S}_E$ and $\delta^{34}\text{S}_{Py}$ respectively. Despite a
220 typically wide range in pyrite sulfur isotope compositions, such as a $\sim 50\text{‰}$ range in Cretaceous
221 pyrite $\delta^{34}\text{S}$ data⁴⁰, the strong $\delta^{34}\text{S}$ difference between average marine evaporite and pyrite is
222 forgiving when using estimated values to partition their mass balance. With the given
223 constraints, the mixing equation becomes:

$$224 \quad \delta^{34}\text{S}_{RW} = f_{Py} * \delta^{34}\text{S}_{Py} + (1 - f_{Py}) * \delta^{34}\text{S}_E \quad (5)$$

225 The mass balance of pyrite and evaporite can then be solved for the unknown fraction of pyrite,
226 f_{Py} , which is determined as 0.72 with evaporite being the remainder. Thus, the sulfate load from
227 rock weathering in the Mississippi River is 72% pyrite-derived sulfate and 28% evaporite sulfate,
228 or a respective 26.5% and 11% of the total Mississippi River sulfate budget (Table S3). A scaling
229 of coal production to riverine sulfate load¹⁵ was previously used to estimate the contribution of
230 mine drainage pyrite-derived sulfate. The result was, out of a total flux of $27.8 \text{ Tg SO}_4^{2-} \text{ yr}^{-1}$
231 from the Mississippi River, sulfate from mine drainage accounted for 47% and its average $\delta^{34}\text{S}$
232 value was estimated as -1.8‰ ³. Thus, the sulfate load from natural and anthropogenically
233 enhanced weathering of shale pyrite and pyrite weathering in mine drainage is $74 \pm 10\%$, or 20.6
234 $\text{Tg SO}_4^{2-} \text{ yr}^{-1}$. Under such heavy loads of pyrite-derived sulfate, the oxygen isotopes of
235 Mississippi River sulfate should strongly reflect variations in the ambient water oxygen source
236 and the pathway of pyrite oxidation.

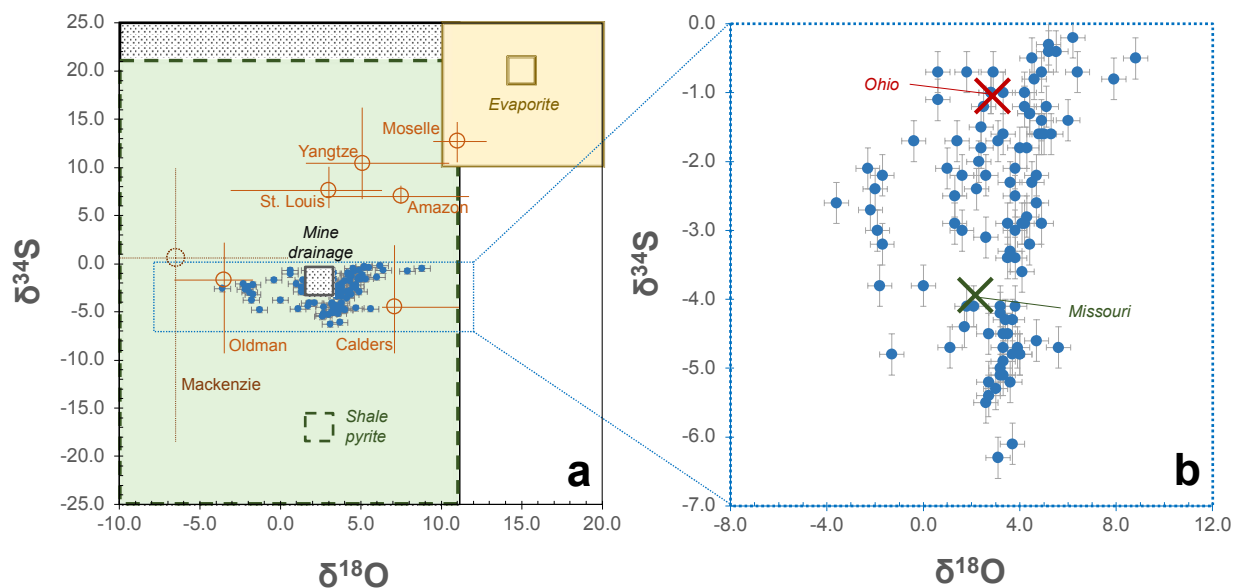
237

238 **Seasonal variations**

239 The differences in sulfur isotope compositions of average bedrocks in Mississippi River
240 sub-basins, and the dominance of pyrite-derived sulfate, may explain the $\delta^{34}\text{S}_{\text{SO}_4}$ seasonality as
241 well as the lack of the same in $\delta^{18}\text{O}_{\text{SO}_4}$ (Figs. 2 and 3), all despite a heavy anthropogenic

242 overprint. A global comparison of riverine sulfate reveals smaller ranges of average $\delta^{18}\text{O}_{\text{SO}_4}$ with
243 high contributions from evaporite sulfate and a larger range of average $\delta^{18}\text{O}_{\text{SO}_4}$ in rivers with
244 higher amounts of pyrite-derived sulfate (shale pyrite and mine drainage sources) (Fig. 3a). Also
245 observed in figure 3a, rivers with high pyrite-derived sulfate loads have $\delta^{18}\text{O}_{\text{SO}_4}$ corresponding to
246 local meteoric water differences, whereas sulfate from the North American Mackenzie, Oldman,
247 and Mississippi Rivers plot with respectively lower to higher $\delta^{18}\text{O}_{\text{SO}_4}$ values that reflect the
248 correlation of lower $\delta^{18}\text{O}_{\text{water}}$ with higher latitudes. The Mississippi River $\delta^{34}\text{S}_{\text{SO}_4}$ and $\delta^{18}\text{O}_{\text{SO}_4}$
249 data indicate the strong signature of pyrite-derived sulfate as compared to evaporite sulfate, and
250 mixing of two sources that are significantly different in their $\delta^{34}\text{S}_{\text{SO}_4}$ but not in their $\delta^{18}\text{O}_{\text{SO}_4}$ (Fig.
251 3b). The Ohio and Missouri River sub-basins contribute a respective 33% and 41% of average
252 Mississippi River sulfate flux during the study period. The average Mississippi River $\delta^{34}\text{S}_{\text{SO}_4}$ and
253 $\delta^{18}\text{O}_{\text{SO}_4}$ for the upper ranges of Ohio and Missouri sulfate flux contributions are plotted in figure
254 3b and indicate that the most important source of ^{34}S -depleted sulfate in the Mississippi River
255 comes from the Missouri River sub-basin³. Source mixing in the Mississippi River is also
256 apparent in a bimodal distribution of $\delta^{34}\text{S}_{\text{SO}_4}$ data with modes at around -1‰ and -5‰ (Fig.
257 S3). During the periods of seasonally low $\delta^{34}\text{S}_{\text{SO}_4}$ the Missouri River accounts for up to $\sim 80\%$ of
258 total Mississippi River sulfate flux (Fig. S4). Sulfate measurements from 01/27/11 to 06/01/11
259 from the upper Ohio River at Tell City, Indiana (Table S2) show that the Ohio has higher
260 average $\delta^{34}\text{S}_{\text{SO}_4}$ (0.3‰) compared to the Mississippi River (-3.2‰) during the same interval.
261 Meanwhile, from figure 3b we estimate that the difference in $\delta^{18}\text{O}_{\text{SO}_4}$ between Ohio and
262 Missouri river sulfate is less than 1‰ .

263



264

265 **Figure 3.** Sulfate $\delta^{34}\text{S}$ is plotted against $\delta^{18}\text{O}$ for this study, selected rivers, and expected ranges
 266 of riverine sulfate sources. In plot (a), sulfate data for the Mississippi River from this study
 267 (filled circles) are shown along with previously published river averages and their ranges (open
 268 circles and error bars for ranges)^{9, 10, 22, 24, 43-45}, and the important rock sources of sulfate of
 269 evaporites⁹, shale pyrite⁴², mine drainage³, with their averages (open squares) and respective
 270 ranges (shaded boxes). Note that the Mackenzie River average is from spatial data while all other
 271 riverine sulfate averages are from time series. The average $\delta^{18}\text{O}_{\text{SO}_4}$ of sulfate derived from
 272 oxidation of pyrite in shales and mine drainage in (a), are estimated from oxygen sources of
 273 average Mississippi River water (-6.6‰ ⁴⁶) and air O_2 (23.5‰ ⁴⁷), with a typical fractionation
 274 between sulfate and water of 9‰ ⁴⁸, and the resulting sulfate oxygen having a source ratio $\frac{3}{4}$
 275 water and $\frac{1}{4}$ air O_2 ⁴⁹. The estimated $\delta^{18}\text{O}_{\text{SO}_4}$ ranges ($\sim -20\text{‰}$ to 11‰) for sulfate from pyrite
 276 oxidation and mine drainage assume that such sulfate can approach a 100% water oxygen end
 277 member ($\sim -20\text{‰}$ at its lowest for US river waters⁵⁰); and on the high end, with US river waters
 278 up to $\sim -2\text{‰}$ ⁵⁰, sulfate could reach up to 11‰ with the aforementioned sulfate-water fractionation
 279 factor and oxygen source ratio. Plot (b) shows an expanded view of the Mississippi River sulfate
 280 data and its averages (large symbols) for the upper 25% of flux contributions from the Ohio and
 281 Missouri Mississippi River sub-basins with respect to the Mississippi River sulfate total.
 282

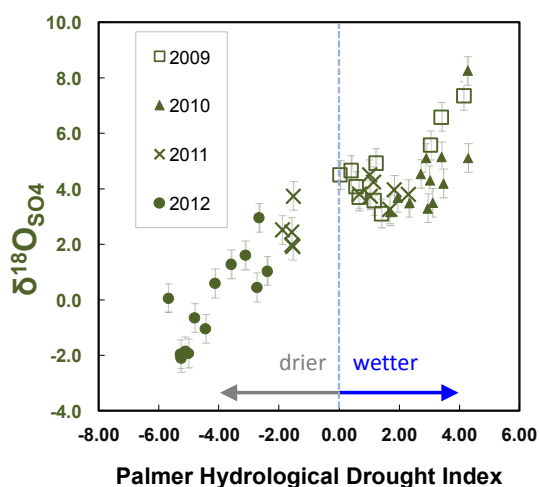
283

284 Differential response of $\delta^{34}\text{S}_{\text{SO}_4}$ and $\delta^{18}\text{O}_{\text{SO}_4}$ to sulfate origin

285 Riverine sulfate oxygen isotope $\delta^{18}\text{O}$ has been used previously to help constrain the
 286 sources of SO_4^{2-} in river systems^{8-10, 51}, however the interpretation of $\delta^{18}\text{O}_{\text{SO}_4}$ is not as
 287 straightforward as $\delta^{34}\text{S}_{\text{SO}_4}$ because $\delta^{34}\text{S}_{\text{SO}_4}$ is able to more faithfully retain source compositions

288 while $\delta^{18}\text{O}_{\text{SO}_4}$ is prone to variable kinetic isotope effects and replacement of its original oxygen⁴⁹,
289 ⁵². The oxygen isotopes of SO_4^{2-} reflect a combination of its sources that are mainly water and
290 air O_2 (where $\delta^{18}\text{O}_{\text{O}_2} = 23.5\text{‰}$ ⁴⁷, and US surface waters range $\sim -20\text{‰}$ to -2‰ in $\delta^{18}\text{O}_{\text{H}_2\text{O}}$ ⁵⁰),
291 oxygen isotope fractionation factors, the net effect of bacterial sulfate reduction, and the
292 pathways of oxidation from sulfide to sulfate. Sulfate generated from the abiotic or biological
293 oxidation of pyrite have $\delta^{34}\text{S}_{\text{SO}_4}$ compositions that are very similar to their pyrite source and
294 $\delta^{18}\text{O}_{\text{SO}_4}$ compositions linked to the $\delta^{18}\text{O}$ of the ambient water source and the oxidation
295 pathway^{53, 54}. Similarly, during the mineralization of biomass the re-oxidation of sulfur will
296 affect the resulting $\delta^{18}\text{O}_{\text{SO}_4}$ and leave $\delta^{34}\text{S}$ relatively unchanged between its sulfur source and
297 the resulting sulfate. Biological sulfur cycling via bacterial sulfate reduction (BSR) and
298 subsequent re-oxidation of the product sulfide to sulfate (for example, in marine environments 75
299 to 90% is re-oxidized⁷) is one of the most significant controls on the mix of oxygen sources in
300 SO_4^{2-} in freshwater and marine environments. Due to BSR, the concentration of remaining SO_4^{2-}
301 decreases and becomes more enriched in ^{18}O and ^{34}S ⁵⁵. During so-called cryptic sulfur cycling,
302 however, BSR can operate without affecting sulfate concentration or $\delta^{34}\text{S}_{\text{SO}_4}$ but a quantitative
303 re-oxidation of sulfide to sulfate results in replacement of sulfate oxygen and thus an effect on
304 $\delta^{18}\text{O}_{\text{SO}_4}$ ⁵⁶. The comparison of sulfate concentrations, $\delta^{18}\text{O}_{\text{SO}_4}$, and $\delta^{34}\text{S}_{\text{SO}_4}$ in the Mississippi
305 River, where pyrite-derived sulfate composes $74 \pm 10\%$ of the budget, may not show conclusive
306 evidence of BSR in the sense of residual sulfate decreasing in concentration and increasing in
307 $\delta^{18}\text{O}_{\text{SO}_4}$ and $\delta^{34}\text{S}_{\text{SO}_4}$. Indeed, the Mississippi River sulfate concentration changes appear related
308 to dilution effects, where spring snowmelt and precipitation result in lower sulfate concentration
309 without a clear signal in $\delta^{18}\text{O}_{\text{SO}_4}$ and $\delta^{34}\text{S}_{\text{SO}_4}$ (Fig. 2).

310 During 2009-2013, Mississippi River $\delta^{18}\text{O}_{\text{SO}_4}$, in contrast to its $\delta^{34}\text{S}_{\text{SO}_4}$, does not respond
 311 seasonally. The $\delta^{18}\text{O}_{\text{SO}_4}$ shows a general decreasing trend concomitant with increasing drought
 312 (Figs. 2 and 4) and a strong peak in the beginning of 2010. The $\delta^{18}\text{O}_{\text{SO}_4}$ response appears to be
 313 basin-wide behavior across the Mississippi River, as compared to the seasonal control on sub-
 314 basin sulfate input reflected in $\delta^{34}\text{S}_{\text{SO}_4}$ variations. First, although it composes just 15% of the
 315 Mississippi River sulfate budget³, the oxygen isotope composition of atmospheric sulfate input is
 316 probably replaced, as consistent with results from a 36-year study in Hubbard Brook where
 317 internal cycling of atmospheric sulfate occurred during a residence time of 9 years^{57, 58}.
 318 Furthermore, there are significant variations in the oxygen isotopes of river water between
 319 Mississippi River sub-basins⁵⁰ and this should register in the Mississippi River that has
 320 significant pyrite-derived sulfate that takes most of its oxygen from water. However, water data
 321 for the Ohio and Upper Mississippi⁵⁹, and Missouri⁶⁰ Rivers, indicates respective average
 322 $\delta^{18}\text{O}_{\text{water}}$ for these rivers of -7.5‰ , -8.2‰ , and -9‰ . The average oxygen isotope differences
 323 are a maximum of 1.5‰ between Mississippi River sub-basin river waters and this will be
 324 reflected in their pyrite-derived sulfate. Thus, while the $\delta^{34}\text{S}_{\text{SO}_4}$ response is strong, the $\delta^{18}\text{O}_{\text{SO}_4}$
 325 responds weakly to the geographic origin of sulfate sources in the Mississippi River (Fig. 3b).



326

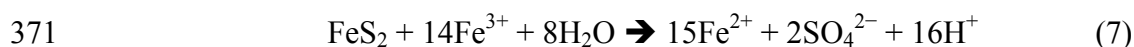
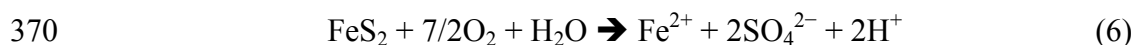
327 **Figure 4.** Monthly averages of Mississippi River sulfate $\delta^{18}\text{O}$, from this study, cross-plotted
328 against monthly Palmer Hydrological Drought Index (PHDI) for the contiguous United States.³⁶
329 Palmer drought indices indicate moisture conditions, with negative and positive values indicating
330 dry and wet anomalies, respectively.⁶¹ In this case, Mississippi River sulfate $\delta^{18}\text{O}$ has a positive
331 correlation with the PHDI, where lower and higher $\delta^{18}\text{O}_{\text{SO}_4}$ correspond to increasing drought and
332 wetter conditions, respectively.

333
334

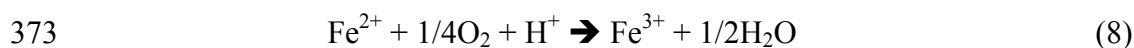
335 **Implications of the trend in $\delta^{18}\text{O}_{\text{SO}_4}$**

336 The trend of decreasing Mississippi River $\delta^{18}\text{O}_{\text{SO}_4}$ over 2009-2013 occurs with increasing
337 average drought and surface temperature in the contiguous United States and this suggests
338 possible mechanisms for the $\delta^{18}\text{O}_{\text{SO}_4}$ response. Monthly averages of Mississippi River sulfate
339 $\delta^{18}\text{O}$ correlate strongly ($R^2 = 0.82$, linear regression) with the Palmer Hydrological Drought
340 Index (PHDI) (Fig. 4). A “hydrological drought” condition is where surface and ground water
341 availability is lower than average due to meteorological drought, as caused by anomalously low
342 precipitation that can in turn be caused by temperature anomalies⁶². The PHDI can be considered
343 an indicator of environmental response to precipitation input, and as such the PHDI changes
344 more slowly than precipitation⁶³. The strong correlation between Mississippi River $\delta^{18}\text{O}_{\text{SO}_4}$ and
345 PHDI, but lack of correlations between $\delta^{18}\text{O}_{\text{SO}_4}$ and changes in sulfate flux between Mississippi
346 River sub-basins or other chemical parameters (e.g., USGS-monitored concentration of redox-
347 sensitive elements such as As and V, water temperature, and dissolved oxygen) suggests that it is
348 a balance between sulfate from more recent surface runoff versus sulfate from groundwater that
349 controls Mississippi River $\delta^{18}\text{O}_{\text{SO}_4}$. It is possible that oxygen source for low $\delta^{18}\text{O}_{\text{SO}_4}$ could be
350 from the northwestern region of the Mississippi River basin, as streamwaters in the upper
351 Missouri River area can range down to a $\delta^{18}\text{O}_{\text{H}_2\text{O}}$ of -18‰ ⁵⁰. However, Mississippi River sulfate
352 should also show the low $\delta^{34}\text{S}_{\text{SO}_4}$ values expected from Missouri River sulfate input if it was
353 more significant during drought but this does not occur (Fig. 2). As reviewed by Van Stempvoort

354 and Krouse⁴⁸, with few exceptions sulfate oxygen isotopes are more ¹⁸O-enriched than the
 355 ambient water in which the sulfate originates due to fractionation between sulfate and water
 356 ($\delta^{18}\text{O} \approx +9\%$) and the variably kinetic incorporation of ¹⁸O-enriched oxygen from air O₂ ($\delta^{18}\text{O} =$
 357 23.5% ⁴⁷). The ¹⁸O-enrichment of sulfate relative to water is due to rapid oxygen exchange
 358 between sulfite and water, where sulfite is an intermediate during sulfide oxidation to sulfate,
 359 and sulfite is shown to be $9.5 \pm 0.8\%$ ¹⁸O-enriched versus water under typical experimental
 360 conditions⁶⁴. While there is some correlation between $\delta^{18}\text{O}_{\text{SO}_4}$ and $\delta^{34}\text{S}_{\text{SO}_4}$ during wetter
 361 conditions (wet PHDI, Fig. S6), during dry conditions there is no such correlation despite nearly
 362 the same range of $\delta^{34}\text{S}_{\text{SO}_4}$ as during wetter conditions in the Mississippi River. Here we suspect a
 363 difference in oxidation pathways for pyrite-derived sulfate in surface versus groundwater
 364 environments, where more extensive weathering of pyrites in groundwater results in a greater
 365 proportion of water oxygen in sulfate as compared to pyrite oxidation in more surficial
 366 environments. Thus, a greater proportion of groundwater sulfate sources, attended by lower
 367 $\delta^{18}\text{O}_{\text{SO}_4}$, may be represented in the river during drought conditions as compared to normal or
 368 high flow periods. As summarized by Taylor and Wheeler, 1993⁶⁵, two reactions are typically
 369 used to describe pyrite oxidation to sulfate:



372 Where reaction (7) is rate-limited by the oxidation of Fe²⁺ by O₂ in the reaction:



374 In experiments⁵³, and in natural systems⁶⁵, it has been observed that the oxidation of pyrite under
 375 submersed and alternating wet/dry conditions results in sulfate with $\delta^{18}\text{O}_{\text{SO}_4}$ that is around 2‰ to
 376 18‰ higher than that of ambient water $\delta^{18}\text{O}_{\text{water}}$, a scenario that was used to estimate the ranges

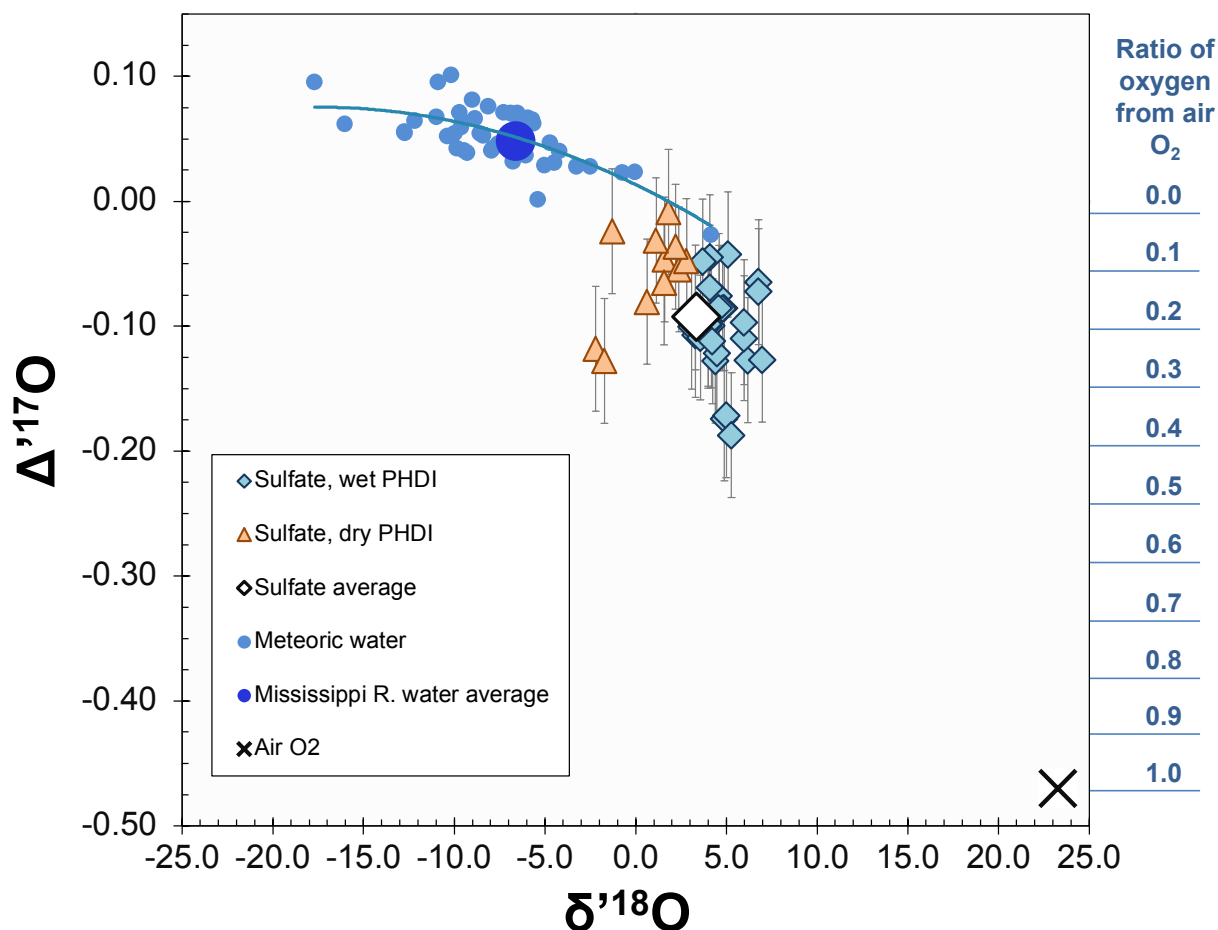
377 of pyrite-derived sulfate for the Mississippi River shown in figure 3a. This $\delta^{18}\text{O}$ offset between
378 pyrite-derived sulfate and water can tend towards a more restricted range of about 5‰ to 12‰ in
379 neutral waters and goes towards smaller offsets (down to $\sim 4\text{‰}$) under submersed, sterile, and
380 anaerobic conditions and larger offsets (up to $\sim 18\text{‰}$) under wet/dry, with sulfide-oxidizing
381 bacteria present, and aerobic conditions⁶⁵. Mississippi River sulfate during drier PHDI conditions
382 may have an even greater proportion of oxygen from water because it is derived from pyrite
383 preferentially oxidized under reaction (7). Alternatively, changing Mississippi River hydrologic
384 conditions may exert a control on an expression of cryptic sulfur cycling within the basin, and
385 thus characteristically affect $\delta^{18}\text{O}_{\text{SO}_4}$ and not $\delta^{34}\text{S}_{\text{SO}_4}$ ⁵⁶, with $\delta^{18}\text{O}_{\text{SO}_4}$ possibly shifting to lower
386 values in accordance with a changing locus of sulfide oxidation from more to less aerated
387 environments, however the mechanisms behind cryptic sulfur cycling are still poorly understood.

388

389 $\Delta^{17}\text{O}_{\text{SO}_4}$ constraints on sulfate oxygen sources

390 Variations in $\Delta^{17}\text{O}_{\text{SO}_4}$ can help to differentiate sources, formation pathways, and
391 processes affecting riverine sulfate. However, $\Delta^{17}\text{O}_{\text{SO}_4}$ in surface waters is an underdeveloped
392 tracer, with presently only one riverine $\Delta^{17}\text{O}_{\text{SO}_4}$ study available⁶⁶. Here we note that $\Delta^{17}\text{O}$ (eq. 2)
393 is used to describe triple oxygen isotopes in general, but we report the logarithmic form $\Delta^{17}\text{O}$
394 (eq. 3). The difference between $\Delta^{17}\text{O}$ and $\Delta^{17}\text{O}_{\text{SO}_4}$ is very small for measurements not far from the
395 origin, for example within error of each other for the Mississippi River sulfate data (Fig. S1).
396 Generally, sulfate has positive $\Delta^{17}\text{O}$ values when originated as secondary atmospheric sulfate,
397 and slightly negative values when formed via oxidation of reduced sulfur⁶⁷. The positive $\Delta^{17}\text{O}$
398 range of atmospheric sulfate, 0.14‰ to 1.43‰ in northern hemisphere precipitation^{68, 69}, is
399 inherited from ozone and/or hydrogen peroxide⁷⁰. This ^{17}O -enrichment from atmospheric SO_4^{2-}

400 input, which is ~15% of the Mississippi River sulfate budget³, is likely lost via replacement with
 401 oxygen from ambient water and/or air O₂ during sulfate reduction and sulfide re-oxidation within
 402 biologically active surface environments. Likewise, the sulfate generated during oxidative
 403 weathering of sulfides, such as pyrite and organic sulfur, will incorporate its oxygen from
 404 ambient water ($\Delta^{17}\text{O} = -0.03$ to $+0.11\text{‰}$ in the Northern Hemisphere⁷¹) and air O₂ ($\Delta^{17}\text{O} =$
 405 -0.47‰ ⁴⁷) with effects from associated fractionation factors.



406
 407 **Figure 5.** Plot of triple oxygen isotopes reported in ‰ VSMOW. The $\Delta^{17}\text{O}$ uses a 0.5305
 408 reference slope and is cross-plotted against $\delta^{18}\text{O}$. All sulfate data are from the Mississippi River
 409 from this study and are shown with values of its potential oxygen sources meteoric water⁷¹ and
 410 air O₂⁴⁷. The average Mississippi River $\delta^{18}\text{O}_{\text{water}}$ is -6.6‰ from the lower Mississippi⁵⁹ and here
 411 its $\Delta^{17}\text{O}$ is inferred. The sulfate data is divided according to wet or dry conditions in the
 412 Mississippi River basin (wet or dry PHDI). The dashed lines schematically represent possible
 413 mixing paths between Mississippi River sulfate oxygen end members, average Mississippi River

414 water and air O₂. The boundaries of this mixing path are based on previous work on δ¹⁸O
415 fractionations between sulfate and water and sulfate and air O₂ during pyrite oxidation^{53, 65}. The
416 location and direction of the arrows indicates starting points for mixing between oxygen end
417 members when the fractionation factors between sulfate and water and sulfate and air O₂ are
418 considered.

419
420 A very simplified view of the triple oxygen isotope composition of Mississippi River
421 sulfate is linear mixing between average Mississippi River water and air O₂. It is tempting to use
422 the δ¹⁸O difference between sulfate and ambient water to assess the relative contributions of
423 water and air O₂ oxygen to sulfate, but the evidence cautions against this. The oxidation of
424 sulfide to sulfate involves multiple kinetic steps that can result in sulfate with a δ¹⁸O value even
425 lower than that of ambient water^{48, 49, 72}. Therefore using δ¹⁸O to estimate water and air O₂
426 oxygen contributions to sulfate may be unreliable, particularly when the sample populations are
427 small. In the case of Δ¹⁷O_{SO4}, it is less prone to the same kinetic effects observed in δ¹⁸O_{SO4}. The
428 use of Δ¹⁷O_{SO4} to assess air O₂ is relevant for understanding the ancient Earth atmosphere in the
429 geological past via sulfate in rocks⁶⁷ and thus characterizing the Δ¹⁷O tracer in modern riverine
430 sulfates is a necessary calibration step. Under the reference frame we use for Δ¹⁷O (where the
431 slope C = 0.5305 in eq. 3), sulfate Δ¹⁷O versus δ¹⁸O will normally show negative correlation
432 when the oxygen sources are water and air O₂ (Fig. 5). As shown in figure 5, the oxygen isotope
433 offset between pyrite-derived sulfate and water that was observed in δ¹⁸O_{SO4} from submersed
434 (closer to water values) and alternating wet/dry experiments (further from water values)⁵³ and in
435 natural settings⁶⁵ appears to also be expressed in the added triple oxygen isotope dimension of
436 Δ¹⁷O. Previous pyrite oxidation experiments using Δ¹⁷O revealed that a stoichiometric average
437 ¼ of oxygen in pyrite-derived SO₄²⁻ came from air O₂ with the remaining ¾ oxygen coming
438 from ambient water⁴⁹. The triple oxygen isotope compositions of water follow a predictable array
439 due to Rayleigh distillation⁷¹. We can use this meteoric water array and the relatively large Δ¹⁷O

440 difference between it and air O₂ to our advantage and estimate if a given sulfate oxygen isotope
 441 composition has an almost entirely water oxygen source by simply checking its closeness to
 442 meteoric water in triple oxygen isotope space (Fig. 5). We assume that the highest Mississippi
 443 River $\Delta^{17}\text{O}_{\text{SO}_4}$ (-0.01‰ , Fig. 5) closely represents the sulfate end member with 100% water
 444 oxygen source because its location in triple oxygen isotope space matches well with the sulfate
 445 predicted from pyrite oxidation, and its attendant oxygen sulfate-water $\delta^{18}\text{O}$ offset, with 100%
 446 water oxygen sourced from average Mississippi River water. The 100% air O₂ sulfate end
 447 member is represented by the value of modern air O₂, $\Delta^{17}\text{O} = -0.47\text{‰}$ ⁴⁷. With these Mississippi
 448 River sulfate oxygen water and air O₂ end members, a mixing equation can be constructed as
 449 follows:

$$450 \quad \Delta^{17}\text{O}_{\text{SO}_4} = f_{\text{airO}_2} * \Delta^{17}\text{O}_{\text{airO}_2} + (1 - f_{\text{airO}_2}) * \Delta^{17}\text{O}_{\text{water}} \quad (9)$$

451 Between these end members, the fraction of air O₂ in Mississippi River sulfate (f_{airO_2}) is 0.18.
 452 Thus, with respect to $\Delta^{17}\text{O}$ and including 1 standard deviation error, $18 \pm 9\%$ of Mississippi
 453 River sulfate oxygen is shown to be sourced from air O₂ (Fig. S7). This result is consistent with
 454 74% of Mississippi River sulfate being from pyrite-derived sulfate. With the assumptions that an
 455 average of 25% of oxygen from air O₂ is in pyrite-derived sulfate⁴⁹, and that all other sulfate
 456 sources sum to $\Delta^{17}\text{O} = 0.00\text{‰}$, then $0.74 * 0.25 = 0.19$, nearly identical, though perhaps
 457 coincidentally so, to the ratio of air O₂ oxygen in Mississippi River sulfate determined via $\Delta^{17}\text{O}$.

458

459 **Modeling the Mississippi River sulfate $\delta^{34}\text{S}$, $\delta^{18}\text{O}$, and $\Delta^{17}\text{O}$ time series**

460 Finally, the Mississippi River sulfate isotope time series were modeled with mixing of
 461 sulfate fluxes between three sub-basins and an input term for PHDI and respectively assigned
 462 isotope values. Twelve inputs are reduced to four variables that are further constrained with our

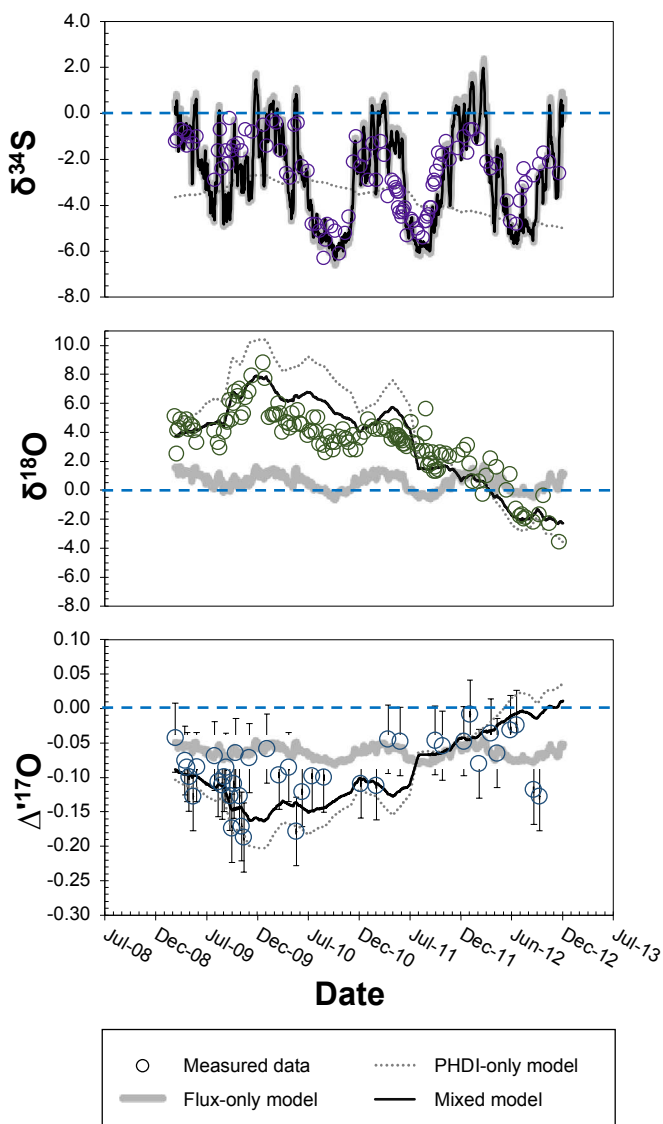
463 sulfate measurements from the Ohio River, published freshwater mussel sulfur isotopes from
 464 within the Mississippi River basin, published water oxygen isotope data, and our updated
 465 Mississippi River sulfate source partitioning. The mixing model is as follows:

$$466 \quad \delta^{xx}Z_{\text{Model}} = f_{\text{Flux}} * (f_{\text{MSR}} * \delta^{xx}Z_{\text{MSR}} + f_{\text{OR}} * \delta^{xx}Z_{\text{OR}} + f_{\text{UMR}} * \delta^{xx}Z_{\text{UMR}}) + f_{\text{PHDI}} * (f_{\text{Wet}} * \delta^{xx}Z_{\text{Wet}} +$$

$$467 \quad f_{\text{Dry}} * \delta^{xx}Z_{\text{Dry}}) \quad (10)$$

468 Here, the $\delta^{xx}Z$ refers to the isotope parameter $\delta^{34}\text{S}$, $\delta^{18}\text{O}$, or $\Delta^{17}\text{O}$; and $\delta^{xx}Z_{\text{Model}}$ is the daily
 469 modeled output for Mississippi River $\delta^{34}\text{S}_{\text{SO}_4}$, $\delta^{18}\text{O}_{\text{SO}_4}$, or $\Delta^{17}\text{O}_{\text{SO}_4}$ during the measured study
 470 period (03/11/09 to 01/01/13). The proportion of influence from the mixing of sulfate fluxes
 471 from Mississippi River sub-basins versus the continental-scale forcing due to overall
 472 hydrological conditions is balanced between f_{Flux} and f_{PHDI} , where $f_{\text{PHDI}} = 1 - f_{\text{Flux}}$. For the mix of
 473 sub-basin sulfate fluxes, f_{MSR} , f_{OR} , and f_{UMR} are the respective sulfate flux ratios and $\delta^{xx}Z_{\text{MSR}}$,
 474 $\delta^{xx}Z_{\text{OR}}$, and $\delta^{xx}Z_{\text{UMR}}$ are the respective isotope values ($\delta^{34}\text{S}_{\text{SO}_4}$, $\delta^{18}\text{O}_{\text{SO}_4}$, or $\Delta^{17}\text{O}_{\text{SO}_4}$) for the
 475 Missouri, Ohio, and Upper Mississippi river sub-basins of the Mississippi River. The sub-basin
 476 fluxes were determined by taking daily water discharge data and matching them with sulfate
 477 concentrations that were interpolated, from measurements taken approximately monthly, to give
 478 daily values. Then, the ratios for sub-basin sulfate fluxes were each sub-basin's sulfate flux
 479 versus their combined sum, here using the mix of sulfate flux between three sub-basins to
 480 represent the whole Mississippi River. The difference in sulfate flux between the averages
 481 determined from the lower Mississippi River and the summed three sub-basins was 6% during
 482 the study period, and thus the flux contribution from the middle Mississippi River is neglected in
 483 the model. The influence of hydrological conditions represented by the Palmer Hydrological
 484 Drought Index is split into “wet” and “dry” components in order to assign different respective
 485 “wet” and “dry” isotope values ($\delta^{xx}Z_{\text{Wet}}$ and $\delta^{xx}Z_{\text{Dry}}$). The PHDI f_{Wet} and f_{Dry} components use

486 reported monthly PHDI interpolated to give daily PHDI, which is then scaled to make a ratio
487 where maximum dry PHDI during the study period is equal to 1, and wet PHDI is the difference,
488 where $f_{\text{Wet}} = 1 - f_{\text{Dry}}$. The model input variables are then $\delta^{\text{xx}}Z_{\text{MSR}}$, $\delta^{\text{xx}}Z_{\text{OR}}$, $\delta^{\text{xx}}Z_{\text{UMR}}$ and f_{Flux} . The
489 input values are explored for feasible Mississippi River $\delta^{34}\text{S}_{\text{SO}_4}$, $\delta^{18}\text{O}_{\text{SO}_4}$, or $\Delta^{17}\text{O}_{\text{SO}_4}$ by testing
490 for the average of sum daily modeled outputs against the average of sum measured values, the
491 correlation between daily model outputs and measured values, and good agreement between the
492 curves of measured and modeled time series data. The best-fitting model outputs are shown in
493 figure 6 and the global values for model parameters are in the supporting information (Table S4).
494 The Mississippi River $\delta^{34}\text{S}_{\text{SO}_4}$ time series model is feasible if the Ohio River has higher $\delta^{34}\text{S}_{\text{SO}_4}$
495 than the Missouri River and it is almost entirely controlled by their balance of sulfate flux input
496 as compared to influence from basinwide wetter or drier conditions, as modeled via PHDI.
497 Mississippi River $\delta^{18}\text{O}_{\text{SO}_4}$ is described well in our model with our estimated contribution of 74%
498 pyrite-derived sulfate dominating sulfate flux and thus resulting in $\delta^{18}\text{O}_{\text{SO}_4}$ that is dominated by a
499 water oxygen source best represented by the average ambient Mississippi River river water $\delta^{18}\text{O}$
500 and a changing oxidation pathway that can be simulated by the PHDI term in the model, whereas
501 only 26% of the Mississippi River $\delta^{18}\text{O}_{\text{SO}_4}$ is due to the balance of sulfate fluxes from the three
502 sub-basins used in the model. The Mississippi River $\Delta^{17}\text{O}_{\text{SO}_4}$ modeling follows the same
503 forcings as $\delta^{18}\text{O}_{\text{SO}_4}$ but there is an additional transient component in the real data which our
504 model is unable to recreate.
505



506

507 **Figure 6.** Time series of modeled Mississippi River $\delta^{34}\text{S}_{\text{SO}_4}$, $\delta^{18}\text{O}_{\text{SO}_4}$, and $\Delta^{17}\text{O}_{\text{SO}_4}$ are shown
 508 with measured data. Measured data error bars are shown or are smaller than symbols. The flux-
 509 only model uses a mix of sulfate flux from three Mississippi River sub-basins, the PHDI-only
 510 model simulates forcing from overall hydrological conditions for the contiguous United States,
 511 and the mixed model incorporates both flux-only and PHDI-only models with further details and
 512 discussion given in the main text.

513

514

515 Implications for riverine sulfate

516 Mississippi River $\Delta^{17}\text{O}_{\text{SO}_4}$, $\delta^{18}\text{O}_{\text{SO}_4}$, and $\delta^{34}\text{S}_{\text{SO}_4}$ each reveal their own different

517 perspectives on the Mississippi River system and its response to seasonal changes or year-to-year

518 weather patterns. Although our Mississippi River study reveals characteristics of riverine sulfate
519 that might be widespread, each river should be considered as a more-or-less unique case, with its
520 own set of processes and sulfur sources dictated by climate, hydrology, and geology. Moreover,
521 in other rivers, anthropogenic influence on sulfate may be expressed by isotopic shifts in the
522 opposite direction, to lower $\delta^{34}\text{S}_{\text{SO}_4}$ for example, as compared to what is inferred from the
523 Mississippi River. Although not done for this study, measurement of the triple oxygen isotope
524 composition ($\delta^{18}\text{O}$ and $\Delta^{17}\text{O}$) of not only the dissolved sulfate, but also the river water from the
525 same sample, could enable high resolution sulfate oxygen isotope mass balance calculations,
526 further assist in tracing river water sources such as runoff versus groundwater, and aid
527 interpretations of the sources of sulfate oxygen and sulfate oxidation pathways. Prime targets for
528 follow-up sulfate sulfur and oxygen isotope studies would be the Missouri and Ohio river sub-
529 basins to characterize the loadings of pyrite-derived sulfate from natural and anthropogenic
530 bedrock weathering and mine drainage. Our results add to the calls for reassessing the
531 contribution of pyrite-derived sulfate to global sulfur budgets⁹, especially pyrite-derived sulfate
532 from coal mining¹⁵, and suggest that the important estimates of natural and anthropogenic global
533 riverine sulfate flux^{5,73} are due for an update.

534

535 **Acknowledgements**

536 Thanks to Bill Alvey and Tell City High School in Indiana for Ohio River water sampling, Justin
537 Hayles, Stefan Lalonde, Manuel Bellanger, Pierre Sans-Jofre, and the members of Bao group
538 past and present for helpful discussions, and the anonymous reviewers whose constructive
539 comments greatly improved this manuscript. National Science Foundation (EAR-1251824, EAR-
540 1312284 to HB) provided part of the research fund, and indirect support was received during the

541 preparation of this manuscript from the European Union Horizon 2020 research and innovation
542 program (Marie Skłodowska-Curie grant agreement No 708117 to BK).

543

544 **Supporting Information Available**

545 Supporting Information includes additional details on methods, modeling, oxygen isotope
546 discussion, and tables of sulfate isotope data, an updated Mississippi River sulfate budget, and
547 model inputs.

548

549 **References**

- 550 1. Canfield, D. E., Sulfur isotopes in coal constrain the evolution of the Phanerozoic sulfur
551 cycle. *Proc. Nat. Acad. Sci. U.S.A.* **2013**, *110*, (21), 8443-6.
- 552 2. Halevy, I.; Peters, S. E.; Fischer, W. W., Sulfate burial constraints on the Phanerozoic
553 sulfur cycle. *Science* **2012**, *337*, (6092), 331-334.
- 554 3. Killingsworth, B. A.; Bao, H., Significant Human Impact on the Flux and $\delta^{34}\text{S}$ of Sulfate
555 from the Largest River in North America. *Environ. Sci. Technol.* **2015**, *49*, (8), 4851-60.
- 556 4. Berner, R. A., Worldwide sulfur pollution of rivers. *J. Geophys. Res.* **1971**, *76*, (27),
557 6597-6600.
- 558 5. Meybeck, M., Concentrations des eaux fluviales en elements majeurs et apports en
559 solution aux oceans. *Rev. Geol. Dyn. Geogr. Phys* **1979**, *21*, (3), 215-246.
- 560 6. Ivanov, M.; Grinenko, V.; Rabinovich, A., Sulphur flux from continents to oceans. In *The*
561 *Global Biogeochemical Sulphur Cycle*, Ivanov, M. V.; Freney, J. R., Eds. John Wiley & Sons,
562 Chichester: 1983; pp 331-356.
- 563 7. Turchyn, A. V.; Schrag, D. P., Oxygen isotope constraints on the sulfur cycle over the
564 past 10 million years. *Science* **2004**, *303*, (5666).
- 565 8. Karim, A.; Veizer, J., Weathering processes in the Indus River Basin: implications from
566 riverine carbon, sulfur, oxygen, and strontium isotopes. *Chem. Geol.* **2000**, *170*, (1), 153-177.
- 567 9. Calmels, D.; Gaillardet, J.; Brenot, A.; France-Lanord, C., Sustained sulfide oxidation by
568 physical erosion processes in the Mackenzie River basin: Climatic perspectives. *Geology* **2007**,
569 *35*, (11), 1003-1006.
- 570 10. Li, X.; Gan, Y.; Zhou, A.; Liu, Y., Relationship between water discharge and sulfate
571 sources of the Yangtze River inferred from seasonal variations of sulfur and oxygen isotopic
572 compositions. *J. Geochem. Explor.* **2015**, *153*, 30-39.
- 573 11. Robinson, B. W.; Bottrell, S. H., Discrimination of sulfur sources in pristine and polluted
574 New Zealand river catchments using stable isotopes. *Appl. Geochem.* **1997**, *12*, (3), 305-319.
- 575 12. Nakano, T.; Tayasu, I.; Wada, E.; Igeta, A.; Hyodo, F.; Miura, Y., Sulfur and strontium
576 isotope geochemistry of tributary rivers of Lake Biwa: implications for human impact on the
577 decadal change of lake water quality. *Sci. Tot. Environ.* **2005**, *345*, (1), 1-12.

- 578 13. Das, A.; Chung, C. H.; You, C. F., Disproportionately high rates of sulfide oxidation
579 from mountainous river basins of Taiwan orogeny: Sulfur isotope evidence. *Geophys. Res. Lett.*
580 **2012**, *39*, (12).
- 581 14. Torres, M. A.; West, A. J.; Clark, K. E.; Paris, G.; Bouchez, J.; Ponton, C.; Feakins, S. J.;
582 Galy, V.; Adkins, J. F., The acid and alkalinity budgets of weathering in the Andes–Amazon
583 system: Insights into the erosional control of global biogeochemical cycles. *Earth Planet. Sci.*
584 *Lett.* **2016**, *450*, 381-391.
- 585 15. Raymond, P. A.; Oh, N.-H., Long term changes of chemical weathering products in rivers
586 heavily impacted from acid mine drainage: Insights on the impact of coal mining on regional and
587 global carbon and sulfur budgets. *Earth Planet. Sci. Lett.* **2009**, *284*, (1), 50-56.
- 588 16. Ingri, J.; Torssander, P.; Andersson, P.; Mörth, C.-M.; Kusakabe, M., Hydrogeochemistry
589 of sulfur isotopes in the Kalix River catchment, northern Sweden. *Appl. Geochem.* **1997**, *12*, (4),
590 483-496.
- 591 17. Fitzhugh, R. D.; Furman, T.; Korsak, A. K., Sources of stream sulphate in headwater
592 catchments in Otter Creek Wilderness, West Virginia, USA. *Hydrol. Processes* **2001**, *15*, (4),
593 541-556.
- 594 18. Björkvald, L.; Giesler, R.; Laudon, H.; Humborg, C.; Mörth, C.-M., Landscape variations
595 in stream water SO₄²⁻ and δ³⁴S SO₄ in a boreal stream network. *Geochim. Cosmochim. Acta*
596 **2009**, *73*, (16), 4648-4660.
- 597 19. Stam, A.; Mitchell, M.; Krouse, H.; Kahl, J., Stable sulfur isotopes of sulfate in
598 precipitation and stream solutions in a northern hardwood watershed. *Water Resour. Res.* **1992**,
599 *28*, (1), 231-236.
- 600 20. Alewell, C.; Mitchell, M.; Likens, G.; Krouse, H., Sources of stream sulfate at the
601 Hubbard Brook Experimental Forest: Long-term analyses using stable isotopes. *Biogeochemistry*
602 **1999**, *44*, (3), 281-299.
- 603 21. Novák, M.; Kirchner, J. W.; Groscheová, H.; Havel, M.; Černý, J.; Krejčí, R.; Buzek, F.,
604 Sulfur isotope dynamics in two central european watersheds affected by high atmospheric
605 deposition of SO_x. *Geochim. Cosmochim. Acta* **2000**, *64*, (3), 367-383.
- 606 22. Otero, N.; Canals, À.; Soler, A., Using dual-isotope data to trace the origin and processes
607 of dissolved sulphate: a case study in Calders stream (Llobregat basin, Spain). *Aquat. Geochem.*
608 **2007**, *13*, (2), 109-126.
- 609 23. Otero, N.; Soler, A.; Canals, À., Controls of δ³⁴S and δ¹⁸O in dissolved sulphate:
610 Learning from a detailed survey in the Llobregat River (Spain). *Appl. Geochem.* **2008**, *23*, (5),
611 1166-1185.
- 612 24. Rock, L.; Mayer, B., Identifying the influence of geology, land use, and anthropogenic
613 activities on riverine sulfate on a watershed scale by combining hydrometric, chemical and
614 isotopic approaches. *Chem. Geol.* **2009**, *262*, (3), 121-130.
- 615 25. Böhlke, J. K.; Michel, R. L., Contrasting residence times and fluxes of water and sulfate
616 in two small forested watersheds in Virginia, USA. *Sci. Tot. Environ.* **2009**, *407*, (14), 4363-
617 4377.
- 618 26. Tichomirowa, M.; Heidel, C.; Junghans, M.; Haubrich, F.; Matschullat, J., Sulfate and
619 strontium water source identification by O, S and Sr isotopes and their temporal changes (1997–
620 2008) in the region of Freiberg, central-eastern Germany. *Chem. Geol.* **2010**, *276*, (1-2), 104-
621 118.
- 622 27. NASA/JPL Shaded Relief with Height as Color, North America.
623 <http://photojournal.jpl.nasa.gov/catalog/PIA03377>

- 624 28. Meybeck, M.; Ragu, A. GEMS/GLORI world river discharge database.
625 <http://doi.pangaea.de/10.1594/PANGAEA.804574>
- 626 29. Goolsby, D. A.; Battaglin, W. A.; Lawrence, G. B.; Artz, R. S.; Aulenbach, B. T.;
627 Hooper, R. P.; Keeney, D. R.; Stensland, G. J. *Flux and sources of nutrients in the Mississippi-*
628 *Atchafalaya River Basin*; National Oceanic and Atmospheric Administration National Ocean
629 Service Coastal Ocean Program: 1999.
- 630 30. Turner, R. E.; Rabalais, N. N., Linking landscape and water quality in the Mississippi
631 River Basin for 200 years. *BioScience* **2003**, *53*, (6), 563-572.
- 632 31. U.S. Geological Survey National Water Information System data available on the World
633 Wide Web (Water Data for the Nation). <http://waterdata.usgs.gov/nwis/>
- 634 32. U.S. Army Corps of Engineers Mississippi River Basin: Stage Data.
635 <http://www2.mvn.usace.army.mil/eng/edhd/wcontrol/miss.asp>
- 636 33. Bao, H., Purifying barite for oxygen isotope measurement by dissolution and
637 reprecipitation in a chelating solution. *Anal. Chem.* **2006**, *78*, (1), 304-309.
- 638 34. Bao, H.; Cao, X.; Hayles, J. A., Triple Oxygen Isotopes: Fundamental Relationships and
639 Applications. *Annu. Rev. Earth Planet. Sci.* **2016**, *44*, (1).
- 640 35. R Core Team *R: A language and environment for statistical computing. R package*
641 *version 3.1.1*, Vienna, 2013.
- 642 36. National Oceanic and Atmospheric Administration (NOAA) National Centers for
643 Environmental Information Climate at a Glance. <http://www.ncdc.noaa.gov/cag/time-series/us/>
- 644 37. Ruhl, L.; Vengosh, A.; Dwyer, G. S.; Hsu-Kim, H.; Deonarine, A.; Bergin, M.;
645 Kravchenko, J., Survey of the Potential Environmental and Health Impacts in the Immediate
646 Aftermath of the Coal Ash Spill in Kingston, Tennessee. *Environ. Sci. Technol.* **2009**, *43*, (16),
647 6326-6333.
- 648 38. Harkness, J. S.; Sulkin, B.; Vengosh, A., Evidence for Coal Ash Ponds Leaking in the
649 Southeastern United States. *Environ. Sci. Technol.* **2016**.
- 650 39. Garrity, C. P., Database of the Geologic Map of North America-Adapted from the Map
651 by JC Reed, Jr. and others (2005). **2009**.
- 652 40. Gautier, D. L., Cretaceous shales from the western interior of North America:
653 Sulfur/carbon ratios and sulfur-isotope composition. *Geology* **1986**, *14*, (3), 225-228.
- 654 41. Fry, B.; Allen, Y. C., Stable isotopes in zebra mussels as bioindicators of river-watershed
655 linkages. *River Res. Appl.* **2003**, *19*, (7), 683-696.
- 656 42. Wortmann, U. G.; Paytan, A., Rapid variability of seawater chemistry over the past 130
657 million years. *Science* **2012**, *337*, (6092), 334-336.
- 658 43. Longinelli, A.; Edmond, J., Isotope geochemistry of the Amazon basin: a reconnaissance.
659 *J. Geophys. Res.: Oceans* **1983**, *88*, (C6), 3703-3717.
- 660 44. Berndt, M.; Bavin, T., On the Cycling of Sulfur and Mercury in the St. Louis River
661 Watershed, Northeastern Minnesota. **2012**.
- 662 45. Brenot, A.; Carignan, J.; France-Lanord, C.; Benoît, M., Geological and land use control
663 on $\delta^{34}\text{S}$ and $\delta^{18}\text{O}$ of river dissolved sulfate: The Moselle river basin, France. *Chem. Geol.* **2007**,
664 *244*, (1), 25-41.
- 665 46. Global Network of Isotopes in Rivers (GNIR) Mississippi River ^{18}O data measured by
666 the USGS Reston laboratory, 1984-1987. [http://www-](http://www-naweb.iaea.org/naweb/ih/IHS_resources_gnir.html)
667 [naweb.iaea.org/naweb/ih/IHS_resources_gnir.html](http://www-naweb.iaea.org/naweb/ih/IHS_resources_gnir.html)
- 668 47. Young, E. D.; Yeung, L. Y.; Kohl, I. E., On the $\Delta^{17}\text{O}$ budget of atmospheric O_2 .
669 *Geochim. Cosmochim. Acta* **2014**, *135*, 102-125.

- 670 48. Van Stempvoort, D.; Krouse, H. In *Controls of $\delta^{18}O$ in sulfate*, Environmental
671 geochemistry of Sulfide Oxidation. Washington DC, American Chemical Society, Symposium
672 Series, 1994; ACS Publications: 1994; pp 446-480.
- 673 49. Kohl, I.; Bao, H. M., Triple-oxygen-isotope determination of molecular oxygen
674 incorporation in sulfate produced during abiotic pyrite oxidation (pH=2-11). *Geochim.*
675 *Cosmochim. Acta* **2011**, *75*, (7), 1785-1798.
- 676 50. Kendall, C.; Coplen, T. B., Distribution of oxygen-18 and deuterium in river waters
677 across the United States. *Hydrol. Processes* **2001**, *15*, (7), 1363-1393.
- 678 51. Turchyn, A. V.; Tipper, E. T.; Galy, A.; Lo, J.-K.; Bickle, M. J., Isotope evidence for
679 secondary sulfide precipitation along the Marsyandi River, Nepal, Himalayas. *Earth Planet. Sci.*
680 *Lett.* **2013**, *374*, 36-46.
- 681 52. Mayer, B., Assessing sources and transformations of sulphate and nitrate in the
682 hydrosphere using isotope techniques. In *Isotopes in the Water Cycle*, Springer: 2005; pp 67-89.
- 683 53. Taylor, B. E.; Wheeler, M. C.; Nordstrom, D. K., Isotope composition of sulphate in acid
684 mine drainage as measure of bacterial oxidation. *Nature* **1984**, *308*, (5959), 538.
- 685 54. Balci, N.; Shanks, W. C.; Mayer, B.; Mandernack, K. W., Oxygen and sulfur isotope
686 systematics of sulfate produced by bacterial and abiotic oxidation of pyrite. *Geochim.*
687 *Cosmochim. Acta* **2007**, *71*, (15), 3796-3811.
- 688 55. Antler, G.; Turchyn, A. V.; Ono, S.; Sivan, O.; Bosak, T., Combined ^{34}S , ^{33}S and ^{18}O
689 isotope fractionations record different intracellular steps of microbial sulfate reduction. *Geochim.*
690 *Cosmochim. Acta* **2017**, *203*, 364-380.
- 691 56. Mills, J. V.; Antler, G.; Turchyn, A. V., Geochemical evidence for cryptic sulfur cycling
692 in salt marsh sediments. *Earth Planet. Sci. Lett.* **2016**, *453*, 23-32.
- 693 57. Likens, G.; Driscoll, C.; Buso, D.; Mitchell, M.; Lovett, G.; Bailey, S.; Siccama, T.;
694 Reiners, W.; Alewell, C., The biogeochemistry of sulfur at Hubbard Brook. *Biogeochemistry*
695 **2002**, *60*, (3), 235-316.
- 696 58. Miles, G. R.; Mitchell, M. J.; Mayer, B.; Likens, G.; Welker, J., Long-term analysis of
697 Hubbard Brook stable oxygen isotope ratios of streamwater and precipitation sulfate.
698 *Biogeochemistry* **2011**, *111*, (1-3), 443-454.
- 699 59. Coplen, T. B.; Kendall, C. *Stable hydrogen and oxygen isotope ratios for selected sites of*
700 *the US Geological Survey's NASQAN and benchmark surface-water networks*; GEOLOGICAL
701 SURVEY RESTON VA: 2000.
- 702 60. Winston, W.; Criss, R., Oxygen isotope and geochemical variations in the Missouri
703 River. *Environ. Geol.* **2003**, *43*, (5), 546-556.
- 704 61. Palmer, W. C., *Meteorological drought*. US Department of Commerce, Weather Bureau
705 Washington, DC, USA: 1965; Vol. 30.
- 706 62. Van Loon, A. F., Hydrological drought explained. *Wiley Interdiscip. Rev.: Water* **2015**, *2*,
707 (4), 359-392.
- 708 63. Heim Jr, R. R., A review of twentieth-century drought indices used in the United States.
709 *Bull. Am. Meteorol. Soc.* **2002**, *83*, (8), 1149.
- 710 64. Wankel, S. D.; Bradley, A. S.; Eldridge, D. L.; Johnston, D. T., Determination and
711 application of the equilibrium oxygen isotope effect between water and sulfite. *Geochim.*
712 *Cosmochim. Acta* **2014**, *125*, 694-711.
- 713 65. Taylor, B. E.; Wheeler, M. C., Sulfur- and Oxygen-Isotope Geochemistry of Acid Mine
714 Drainage in the Western United States. In *Environmental Geochemistry of Sulfide Oxidation*,
715 American Chemical Society: 1993; Vol. 550, pp 481-514.

- 716 66. Johnson, C. A.; Mast, M. A.; Kester, C. L., Use of $^{17}\text{O}/^{16}\text{O}$ to trace atmospherically -
717 deposited sulfate in surface waters: A case study in Alpine watersheds in the Rocky Mountains.
718 *Geophys. Res. Lett.* **2001**, *28*, (23), 4483-4486.
- 719 67. Bao, H., Sulfate: A time capsule for Earth's O_2 , O_3 , and H_2O . *Chem. Geol.* **2015**, *395*,
720 108-118.
- 721 68. Jenkins, K. A.; Bao, H., Multiple oxygen and sulfur isotope compositions of atmospheric
722 sulfate in Baton Rouge, LA, USA. *Atmos. Environ.* **2006**, *40*, (24), 4528-4537.
- 723 69. Li, X.; Bao, H.; Gan, Y.; Zhou, A.; Liu, Y., Multiple oxygen and sulfur isotope
724 compositions of secondary atmospheric sulfate in a mega-city in central China. *Atmos. Environ.*
725 **2013**, *81*, 591-599.
- 726 70. Savarino, J.; Lee, C. C.; Thiemens, M. H., Laboratory oxygen isotopic study of sulfur
727 (IV) oxidation: Origin of the mass - independent oxygen isotopic anomaly in atmospheric
728 sulfates and sulfate mineral deposits on Earth. *J. Geophys. Res.: Atmos.* **2000**, *105*, (D23),
729 29079-29088.
- 730 71. Luz, B.; Barkan, E., Variations of $^{17}\text{O}/^{16}\text{O}$ and $^{18}\text{O}/^{16}\text{O}$ in meteoric waters. *Geochim.*
731 *Cosmochim. Acta* **2010**, *74*, (22), 6276-6286.
- 732 72. Tichomirowa, M.; Junghans, M., Oxygen isotope evidence for sorption of molecular
733 oxygen to pyrite surface sites and incorporation into sulfate in oxidation experiments. *Appl.*
734 *Geochem.* **2009**, *24*, (11), 2072-2092.
- 735 73. Berner, E. K.; Berner, R. A., *Global environment: water, air, and geochemical cycles.*
736 Princeton University Press: 2012.
737

738

